Supporting Information

Chen et al. 10.1073/pnas.1015397108

SI Materials and Methods

Growth Conditions. *Escherichia coli* and *Caulobacter crescentus* strains were grown as described previously (1). Strains, plasmids, and primers used in this study are listed in Table S1. All plasmids were introduced into *C. crescentus* by electroporation or by conjugation with *E. coli* S17 cells as described previously (2). PCR amplification of genes and promoters from CB15N genomic DNA was performed under previously described conditions (1).

For analysis of synchronized populations, mixed populations were grown in peptone-yeast extract (PYE) and induced and synchronized using Percoll density centrifugation as previously described (3). Synchronized swarmer cells were resuspended in PYE to an OD_{600} of 0.2–0.3. For movies of mixed populations, cells were grown in PYE to an OD_{600} of 0.2–0.3. Synchronized swarmer or mixed population cells were spotted onto 1.2–1.5% agarose (UltraPure Agarose; Invitrogen) PYE pads containing 0.3% xylose. Cephalexin (36 μg/mL) was added to the pads when indicated.

Strain Construction. To construct *C. crescentus* strain ML1753, ϕCr30-based transduction of a chloramphenicol-marked, temperature sensitive *divL(A288V)* allele (*divL*^{ts}) (4) from ML1798 was used to replace wild-type chromosomal *divL* in the fluorescent repressor-operator system (FROS) strain (MT16) (5). To construct strain ML1798, a C-terminal fragment of *divL(A288V)* was amplified from PC4403 with primers divLfulllengthrev and divLfwd1788 (4). The PCR product was digested with EcoRI and KpnI and ligated into those sites in pMCS6, a chloramphenicol-marked integration vector (6). The resulting plasmid (pMCS6:*divL(A288V)*) was electroporated into CB15N.

To construct strain ML1754, 1261 bp of *cckA(V366P)* were amplified from pML83:P_{xyl}-*cckA(V366P)* with primers CckA_EcoRI_Fw and CckA_HindIII_Rev, which added a 5′ EcoRI site and 3′ HindIII site. This fragment of *cckA(V366P)* was then TOPO cloned into pCR2.1-TOPO (Invitrogen), sequenced, and then digested with EcoRI and HindIII and ligated into the integration vector pNPTS138, also digested with EcoRI and HindIII. The resulting plasmid pNPTS138-*cckA(V366P)* was electroporated into the FROS strain (MT16). Clones in which the plasmid had recombined were counterselected on sucrose and screened by sequencing of the *cckA* gene for the correct markerless replacement of wild-type *cckA* with the mutant allele.

To construct strain ML1756, a C-terminal fragment of *divL* without the stop codon was amplified by PCR with primers divLfulllengthrev and divLfwd1788. The *divL* PCR product was cloned in frame with the *egfp* gene in pGFPC-4 using KpnI and EcoRI restriction sites. The plasmid was recombined into CB15N by electroporation to generate chromosomally encoded *divL-egfp*.

To construct strains ML1793 and ML1794, the *tetO* cassette in MT16 was first PCR amplified using primers CC0006_HindIII_fw and M13R_EcoRI. This PCR product was digested with HindIII and EcoRI and ligated into the *Caulobacter* integration vector pNPTS138, also digested with HindIII and EcoRI. The resulting plasmid pNPTS138:*cc0006-tetO* was electroporated into the origin mutant "bc_Ld" strain GM3193 and "bd" strain GM3103 (7). A ϕCr30-based transduction with phage lysate from MT16 and selection on spectinomycin was then used to insert *lacI-ECFP-tetR-EYFP* at the *xylX* locus.

To construct strain ML1876, P_{xyl}-*ftsZ*::kan was transduced from YB1585 (8) into a strain containing the *tetO* cassette at the origin and P_{van}-*tetR-YFP* at the *vanA/B* locus.

Flow Cytometry. Wild-type CB15N were grown in PYE, and wild-type *E. coli* K12 were grown in LB. At time 0, cephalexin (36 μg/mL) was added to both *Caulobacter* and *E. coli* cultures to stop cell division. Rifampicin (60 μg/mL for *Caulobacter*, 300 μg/mL for *E. coli*) was then added to cultures at either $t = 0$ to prevent new rounds of DNA replication or at a later time to allow for one additional round of replication in division-inhibited cells (60 min for *Caulobacter* and 15 min for *E. coli*). After rifampicin addition, cells were incubated at 30 °C for 4 h (*Caulobacter*) or at 37 °C for 3 h (*E. coli*) to allow for completion of ongoing rounds of replication before sample collection. Processing and flow cytometry of samples was performed as previously described for *Caulobacter* (9) and *E. coli* (10).

Pulse-Chase Analyses. For determining CtrA half-life, cultures of ML1506, which contains *ctrA* driven by a xylose-inducible promoter on a medium-copy plasmid, were grown in M2G at 30 °C until OD_{600} reached ≈0.3. Expression of plasmid-encoded *ctrA* was then induced with 0.03% xylose for 1.5 h before synchronization. For measurement of CtrA half-life, a synchronized culture was either pulse-labeled immediately after release into M2G or grown for 120 min in M2G supplemented with cephalexin (36 μg/mL) before pulse-labeling. Cells were pulsed for 2 min with 10 μCi ml^{-1} [^{35}S]-methionine and then chased with excess cold methionine and casamino acids. Culture (1 mL) was collected at each time point indicated and flash-frozen in liquid nitrogen. After resuspending cell pellets in 50 mL SDS buffer and boiling for 2 min, the cell lysate was resuspended in 800 mL IP wash buffer [50 mM Tris-HCl (pH 8), 150 mM NaCl, 1 mM EDTA, and 0.5% Triton X-100] and precleared with 25 μL Staph A cells (Calbiochem) for 10 min on ice. Each sample was then spun down and the precleared supernatant transferred to a new tube. CtrA antiserum (Covance) was added at a dilution of 1:550 and rocked gently at 4 °C overnight; 30 μL protein A-agarose (Invitrogen) was then added for 1 h. The immunoprecipitate was collected by centrifugation, washed three times with IP wash buffer, resuspended in 15 μL of SDS sample buffer, and boiled for 4 min. The resulting samples were resolved by SDS/PAGE. The gel was dried and exposed against a Phosphor Screen (Molecular Dynamics) for at least 5 d. Labeled protein bands were scanned and quantified using a PhosphorImager with ImageQuant software (Molecular Dynamics).

Determination of the phosphoryl group half-life of CtrA∼P was done as previously described (11) with the following modifications. A synchronized culture of the wild-type FROS strain (MT16) was grown in M5G for 80 min until they had reached the predivisional stage. The cells were then labeled for 5 min with 90 μCi [γ^{32}P]-ATP per milliliter of culture and the first sample collected. After labeling, the cells were chased with an excess of cold ATP (1 mM). Samples were then immunoprecipitated using CtrA antiserum (Covance).

Fluorescence Recovery After Photobleaching Analyses. Fluorescence recovery after photobleaching (FRAP) experiments were performed on a Nikon Eclipse Ti-E inverted microscope with a Nikon Plan Apo 100× objective (numerical aperture of 1.4) and a Haison Plexiglas chamber heated with an Air-Therm Atx heater to maintain cells at 30 °C. Images were recorded with an Andor DU-885 camera. A 405-nm solid state Ixon laser passed through a Chroma CFP filter cube was used for illumination. The laser formed a Gaussian spot with a full-width-half-maximum size of ≈3 μm. Cells constitutively expressing YFP-CtrA were grown on agarose pads containing cephalexin for 90 min and then imaged. YFP-CtrA levels in each cell was measured with a 1-s exposure, followed by

bleaching of a polar region with the laser for 200 ms. YFP-CtrA levels were then measured every second (with 1-s exposures) for 9 s to assess recovery. Forty-seven cells were analyzed, and a representative cell is shown in Fig. S1*C*. For comparison, a cell in which compartmentalization had already occurred is shown in Fig. S1*D*. All imaging and FRAP was done with an ND8 filter. Image analysis was done in Excel and Matlab using a modified version of PSICIC (http://www.molbio1.princeton.edu/labs/gitai/psicic/psicic.html).

Determination of Cell Length. To measure cell lengths, a freehand line in ImageJ (http://rsbweb.nih.gov/ij/) was drawn through the middle of the cell running from the pole to pole. The pixel length of this line was then converted to millimeters according to the magnification used.

Reaction–Diffusion Model of CtrA∼P Dynamics. Our reaction–diffusion model of the CckA/DivL/CtrA system is described in the main text (*Materials and Methods*). Additional details are provided here.

To model the effects of ChpT on CtrA∼P asymmetry, we treat $\sigma_k = 100$/s and $\sigma_p = 10$/s as the phosphotransfer rates between CckA and ChpT and assume that phosphotransfer between ChpT and CtrA occurs at the poles at the rate 100/s. We assume that the concentration of ChpT is significantly higher than CckA, such that ChpT is not a bottleneck for CtrA phosphorylation. When ChpT spends a significant fraction of the time bound to CckA, the phosphorylation and dephosphorylation of CtrA again occurs predominantly at the poles, and there is a linear gradient of CtrA∼P with higher levels of CtrA∼P at the swarmer pole. If ChpT is free to diffuse, CckA produces opposing linear gradients of ChpT and ChpT∼P, identical to the gradients of CtrA and CtrA∼P in Fig. 2*A* (main text). These gradients of CtrA phosphorylation and dephosphorylation are still able to maintain an asymmetric distribution of CtrA∼P (Fig. S4*A*), with similar effects to delocalizing the kinase activity of CckA (Fig. S6*B*).

If the population of CtrA is very large, the CckA population could saturate, reducing the kinase and phosphatase rates in a CtrA and CtrA∼P concentration-dependent manner, respectively. In Fig. S6*E*, we incorporate saturation of CckA at high CtrA concentration by multiplying σ_k and σ_p by $(1 + [\mathrm{CtrA}]/K)^{-1}$ and $(1 + [\mathrm{CtrA{\sim}P}]/K)^{-1}$, respectively, where K is 10% of the total amount of CtrA. We verified that saturation has little effect on a gradient (Fig. S6*E*), because the concentrations of CtrA and CtrA∼P are kept low at the swarmer and stalked poles, respectively, by the activities of CckA.

Markov Model of CtrA∼P Replication Inhibition. If CtrA∼P is the only determinant of the timing of origin firing, the average duration before firing events is determined by the steady-state densities at the poles. To determine the dependence of replication asymmetry on the number of CtrA∼P binding sites, we varied the number of independent binding sites n_b between two and four binding sites [sites a and b are cooperative and hence treated as a single site (12)] and assumed that binding of CtrA∼P to any one site is sufficient to inhibit replication initiation. Given a CtrA population of 10,000 molecules, the number of CtrA∼P molecules available to bind to the origin within a volume of $(50\ \mathrm{nm})^3$ is between 0 and 20, depending on the gradient of concentration in Fig. 2*A* (main text). We selected rates of CtrA∼P binding (σ_b) and unbinding (σ_u) to match the average time of initiation in wild-type cells. We assumed that replication initiates rapidly as soon as all binding sites are empty. This selection of DNA-binding volume and rate constants illustrates the qualitative dependence of firing time on the number of binding sites, although other pairs of values (σ_b, σ_u) and numbers of CtrA∼P also produce the same initiation time. We ignored diffusion within this volume given that comparatively slow time scales of binding are required to reproduce measured firing times. The number of sites bound by CtrA∼P was varied stochastically using a Monte Carlo algorithm, and we calculated the probabilities P_i of $i = 1,2,\ldots,n_b$ sites being occupied. The average time before firing in 1,000 simulations (Fig. 3*C* in main text) was determined as $\langle T \rangle = (P_1\sigma_u)^{-1}$, where we have assumed that multiple simultaneous unbinding events is extremely unlikely.

1. Skerker JM, Prasol MS, Perchuk BS, Biondi EG, Laub MT (2005) Two-component signal transduction pathways regulating growth and cell cycle progression in a bacterium: A system-level analysis. *PLoS Biol* 3:e334.
2. Ely B (1991) Genetics of *Caulobacter crescentus*. *Methods Enzymol* 204:372–384.
3. Jones SE, Ferguson NL, Alley MR (2001) New members of the ctrA regulon: The major chemotaxis operon in *Caulobacter* is CtrA dependent. *Microbiology* 147: 949–958.
4. Wu J, Ohta N, Zhao JL, Newton A (1999) A novel bacterial tyrosine kinase essential for cell division and differentiation. *Proc Natl Acad Sci USA* 96:13068–13073.
5. Viollier PH, et al. (2004) Rapid and sequential movement of individual chromosomal loci to specific subcellular locations during bacterial DNA replication. *Proc Natl Acad Sci USA* 101:9257–9262.
6. Thanbichler M, Iniesta AA, Shapiro L (2007) A comprehensive set of plasmids for vanillate- and xylose-inducible gene expression in *Caulobacter crescentus*. *Nucleic Acids Res* 35:e137.
7. Bastedo DP, Marczynski GT (2009) CtrA response regulator binding to the *Caulobacter* chromosome replication origin is required during nutrient and antibiotic stress as well as during cell cycle progression. *Mol Microbiol* 72:139–154.
8. Wang Y, Jones BD, Brun YV (2001) A set of ftsZ mutants blocked at different stages of cell division in *Caulobacter*. *Mol Microbiol* 40:347–360.
9. Chen YE, Tsokos CG, Biondi EG, Perchuk BS, Laub MT (2009) Dynamics of two Phosphorelays controlling cell cycle progression in *Caulobacter crescentus*. *J Bacteriol* 191:7417–7429.
10. Riber L, Løbner-Olesen A (2005) Coordinated replication and sequestration of oriC and dnaA are required for maintaining controlled once-per-cell-cycle initiation in *Escherichia coli*. *J Bacteriol* 187:5605–5613.
11. Jacobs C, Hung D, Shapiro L (2001) Dynamic localization of a cytoplasmic signal transduction response regulator controls morphogenesis during the *Caulobacter* cell cycle. *Proc Natl Acad Sci USA* 98:4095–4100.
12. Siam R, Marczynski GT (2000) Cell cycle regulator phosphorylation stimulates two distinct modes of binding at a chromosome replication origin. *EMBO J* 19:1138–1147.

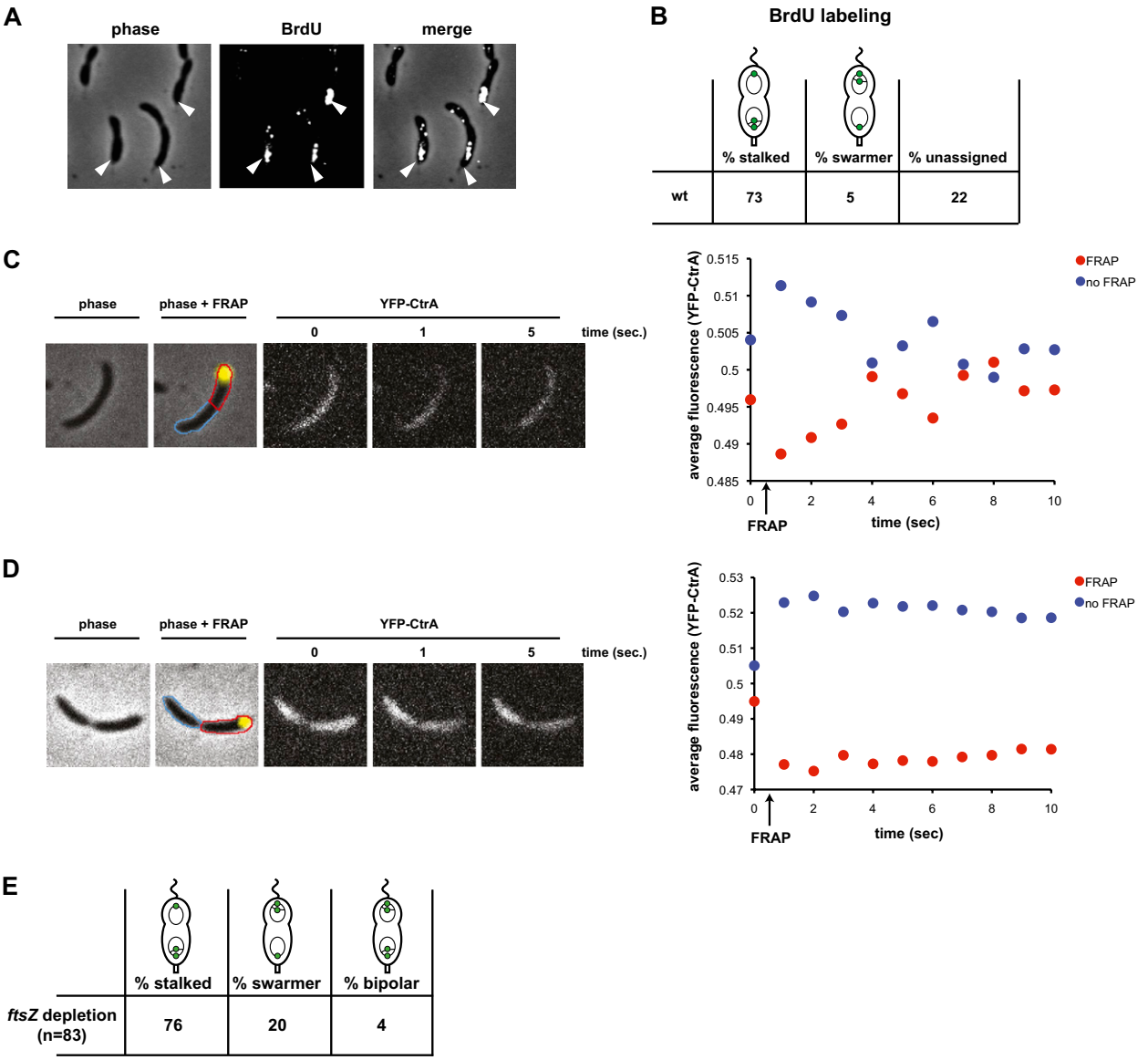

Fig. S1. DNA replication occurs asymmetrically in cells treated with cephalexin or depleted of *ftsZ*. (*A*) Representative immunofluorescence images of asymmetrical BrdU incorporation in the stalked half of wild-type predivisional cells treated with cephalexin. White arrowheads indicate the stalked pole, as determined from the phase micrograph. (*B*) Quantification of BrdU incorporation in cells analyzed by microscopy. (*C*) Fluorescence recovery after photobleaching analysis of a cell expressing YFP-CtrA and growing on an agarose pad containing cephalexin. A phase image of the cell is shown alone and with a yellow dot representing the portion of the cell bleached, followed by fluorescence images taken immediately before and at 1 and 5 s after bleaching. The average fluorescence intensity within the two halves of the cell (indicated with red and blue outlines in the phase image) was measured before bleaching and every second after bleaching. These fluorescent intensities are plotted as a function of time (*Right*). The arrow labeled "FRAP" shows the time of bleaching. A total of 47 cells were examined by FRAP with the majority (>75%) showing similar YFP-CtrA levels in the two halves of the cell within 1–8 s after bleaching, as with the example cell shown here. (*D*) Same as in *C*, but for a cell in which compartmentalization had already occurred before FRAP analysis and cephalexin addition. YFP-CtrA levels in the two halves of the cell do not converge after bleaching one pole. (*E*) Quantification of the spatial patterns of DNA replication in cells depleted of *ftsZ*.

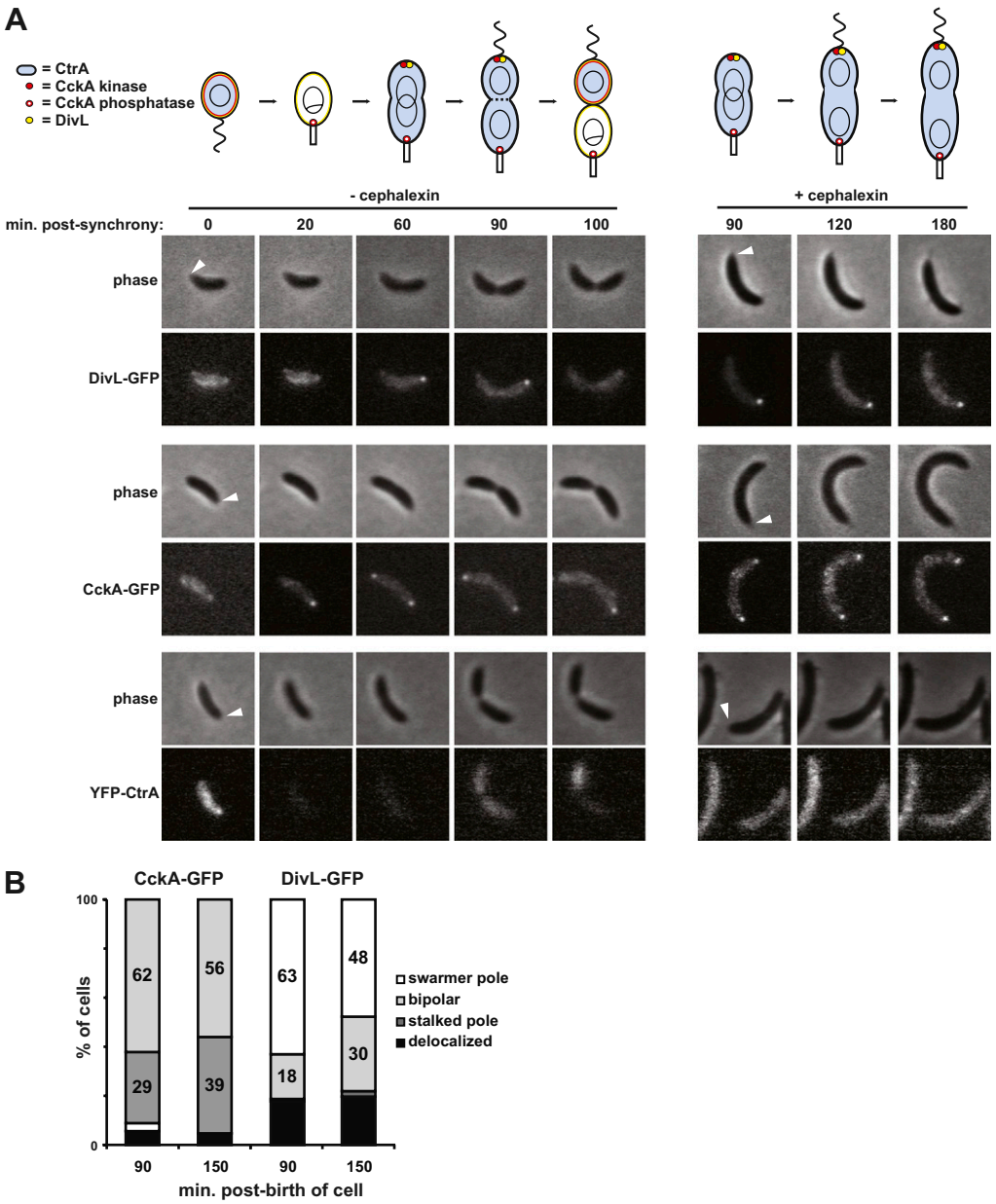

Fig. S2. Cell-cycle dependent localization of DivL, CckA, and CtrA is not altered by cephalexin treatment. (*A*) Schematics (*Upper*) illustrate progression through the cell cycle stages that correspond to the micrographs (*Lower*) and summarize the subcellular localization patterns of CtrA, DivL, and CckA. Synchronized swarmer cells were grown on agarose pads without cephalexin (*Left*) or with cephalexin (*Right*). DivL-GFP is localized to the swarmer pole in late stalked and predivisional cells. DivL-GFP remains localized to the swarmer pole of most cells after cephalexin treatment (*B*). CckA-GFP is localized bipolarly in most predivisional cells. CckA-GFP remains localized to both poles in most cells after cephalexin treatment (*B*). YFP-CtrA is abundant in swarmer cells, eliminated in stalked cells, and abundant again in predivisional cells. After cell division, YFP-CtrA is cleared from the stalked daughter cell. In cells treated with cephalexin, CtrA remains homogenously distributed in predivisional cells. White arrowheads indicate the stalked poles.

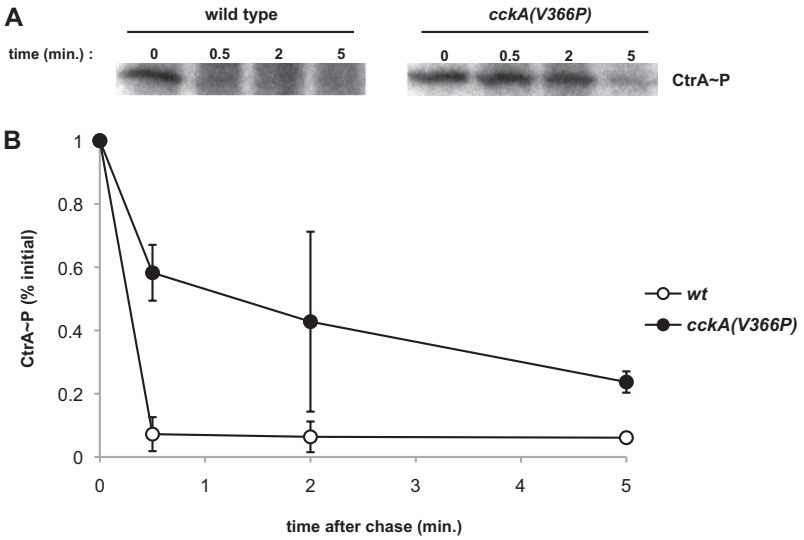

Fig. S3. Kinetics of CtrA~P dephosphorylation in vivo. (*A*) In vivo phosphorylation pulse-chase showing ^{32}P-labeled CtrA (CtrA~P) levels in synchronized predivisional cells from the wild-type strain or from cells expressing *cckA(V366P)*, each grown in M5G. Time 0 is after labeling and immediately before adding the chase solution. All other time points are taken after adding the chase solution. (*B*) Quantification of the CtrA~P bands. Error bars represent SDs calculated from two experiments done on separate days using independent cultures.

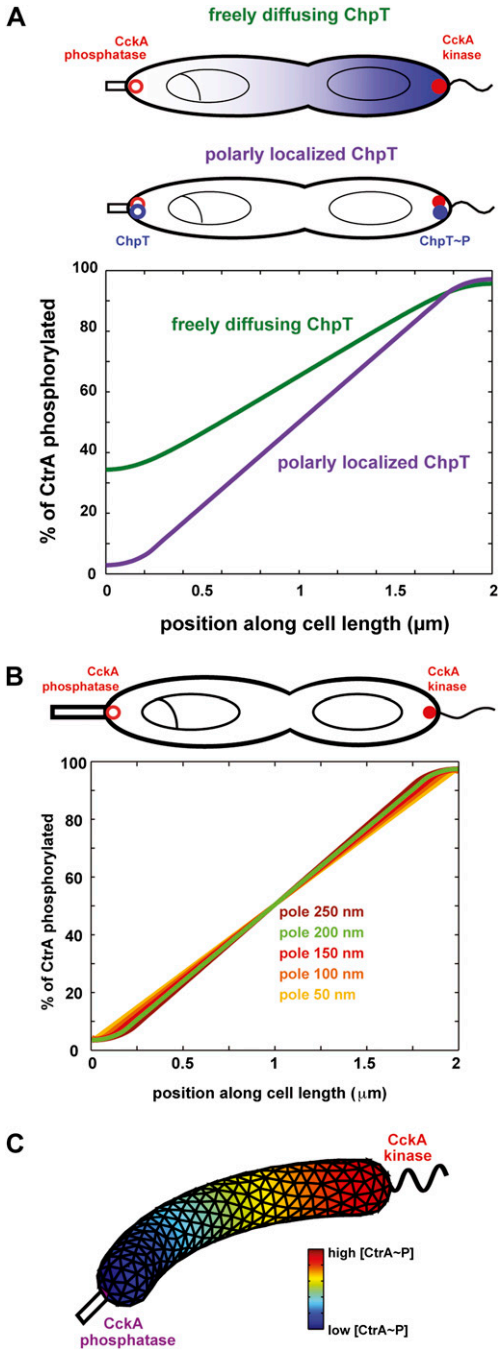

Fig. S4. CtrA~P asymmetry is insensitive to ChpT diffusion and to the size of polar CckA activity. (*A*) Simulations of CtrA phosphorylation gradient when ChpT is included as a freely diffusible species (green line) or polarly localized during phosphotransfer via binding to CckA (purple line). The rates of ChpT phosphorylation and dephosphorylation by CckA are 100/s and 10/s, respectively, and levels of ChpT are chosen so that the rates of CtrA phosphorylation and dephosphorylation at the poles are 100/s. If polarly localized, ChpT-mediated phosphorylation produces a CtrA~P gradient identical to that in Fig. 4*A* (main text). If ChpT diffuses freely, CtrA~P has similar polar concentrations and has a concave distribution. Diagrams above indicate the distribution of ChpT and ChpT~P (blue) engaged in phosphotransfer to CtrA in the two models. (*B*) 1D simulations of the CtrA phosphorylation gradient when the area of CckA activity at the poles was varied between 50 and 250 nm. (*C*) 3D simulation of the CtrA phosphorylation gradient when the area of CckA activity at the poles is restricted to a width of 50 nm.

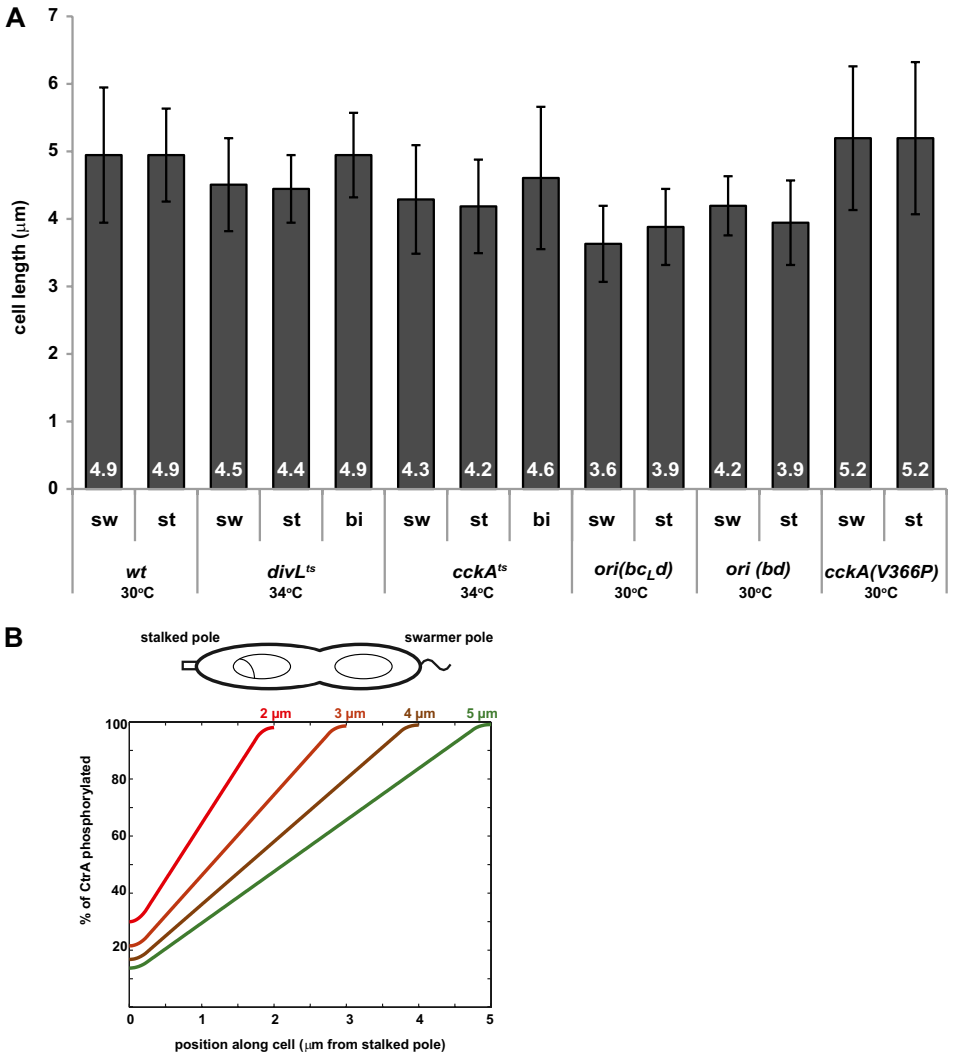

Fig. S5. Cell length at the time of replication does not affect the extent of replicative asymmetry. (*A*) Cell length was measured at the time of replication initiation in predivisional cells in each of the strains indicated. Cells were classified according to whether replication initiated from the swarmer pole (sw), stalked pole (st), or from both poles (bi). The average cell length (μm) is listed at the bottom of each bar. (*B*) Mathematical modeling showing that the spatial asymmetry in CtrA~P concentration is insensitive to cell length, using the wild-type localization and kinetic parameters from Fig. 2*A* (main text).

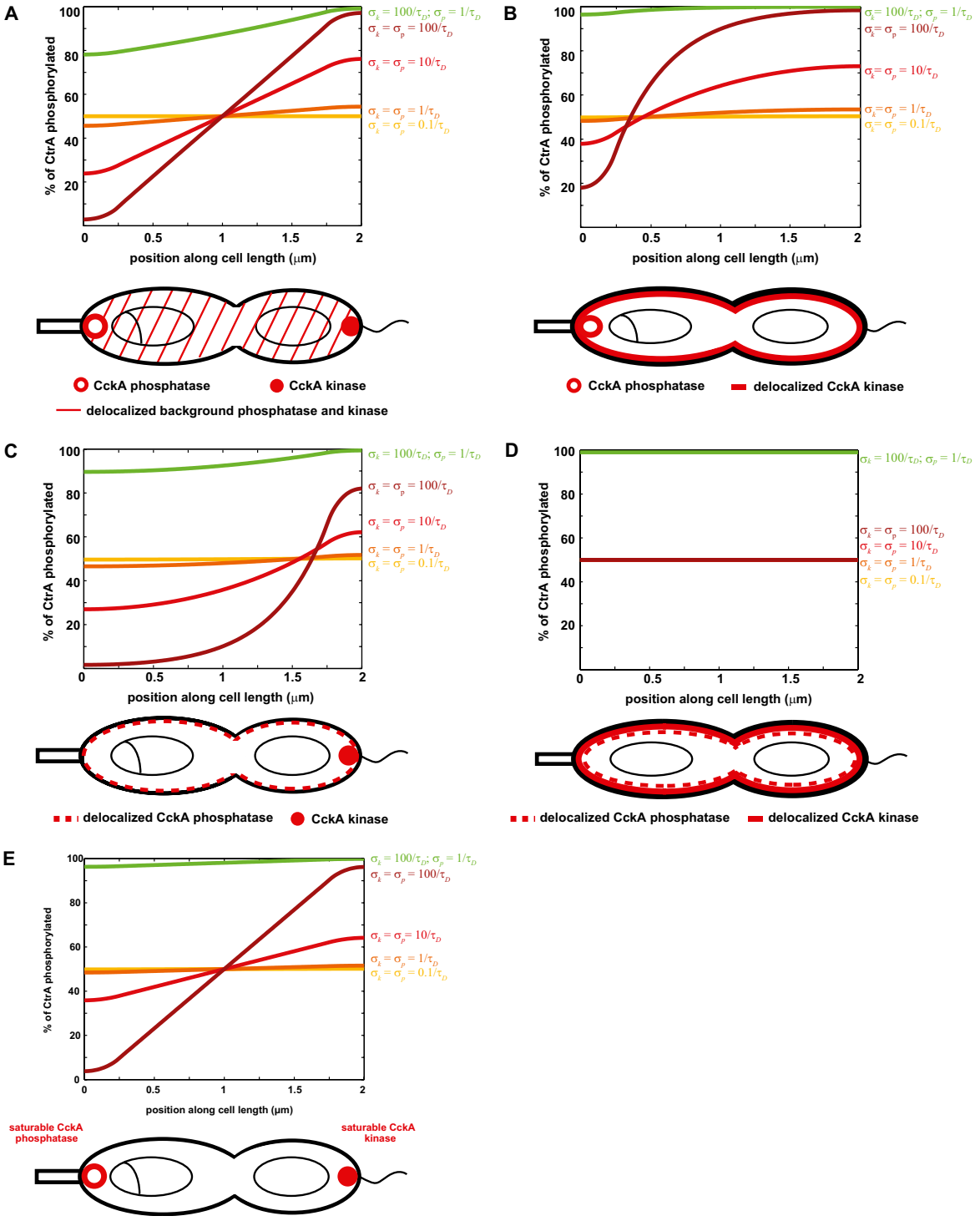

Fig. S6. CtrA∼P asymmetry can be established if either phosphorylation or dephosphorylation, but not both, is delocalized. (*A*) Low levels of delocalized background phosphotransfer activity with rate $0.1/\tau_D$ have little effect on the gradients shown in Fig. 4*A* (main text). (*B* and *C*) A delocalized exogenous kinase (*B*) or phosphatase (*C*) will also generate spatial gradients in CtrA∼P if the phosphorylation and dephosphorylation rates are fast compared with $1/\tau_D$ and the opposing activity remains localized. (*D*) The spatial gradient is completely eliminated when both kinase and phosphatase activity is delocalized. (*E*) Modeling predicts that saturation of the phosphorylation and dephosphorylation of CtrA at 10% of its average cellular concentration (*SI Materials and Methods*) does not abolish the spatial asymmetry in CtrA∼P when the phosphorylation and dephosphorylation rates, σ_k and σ_p, are large compared with $1/\tau_D$.

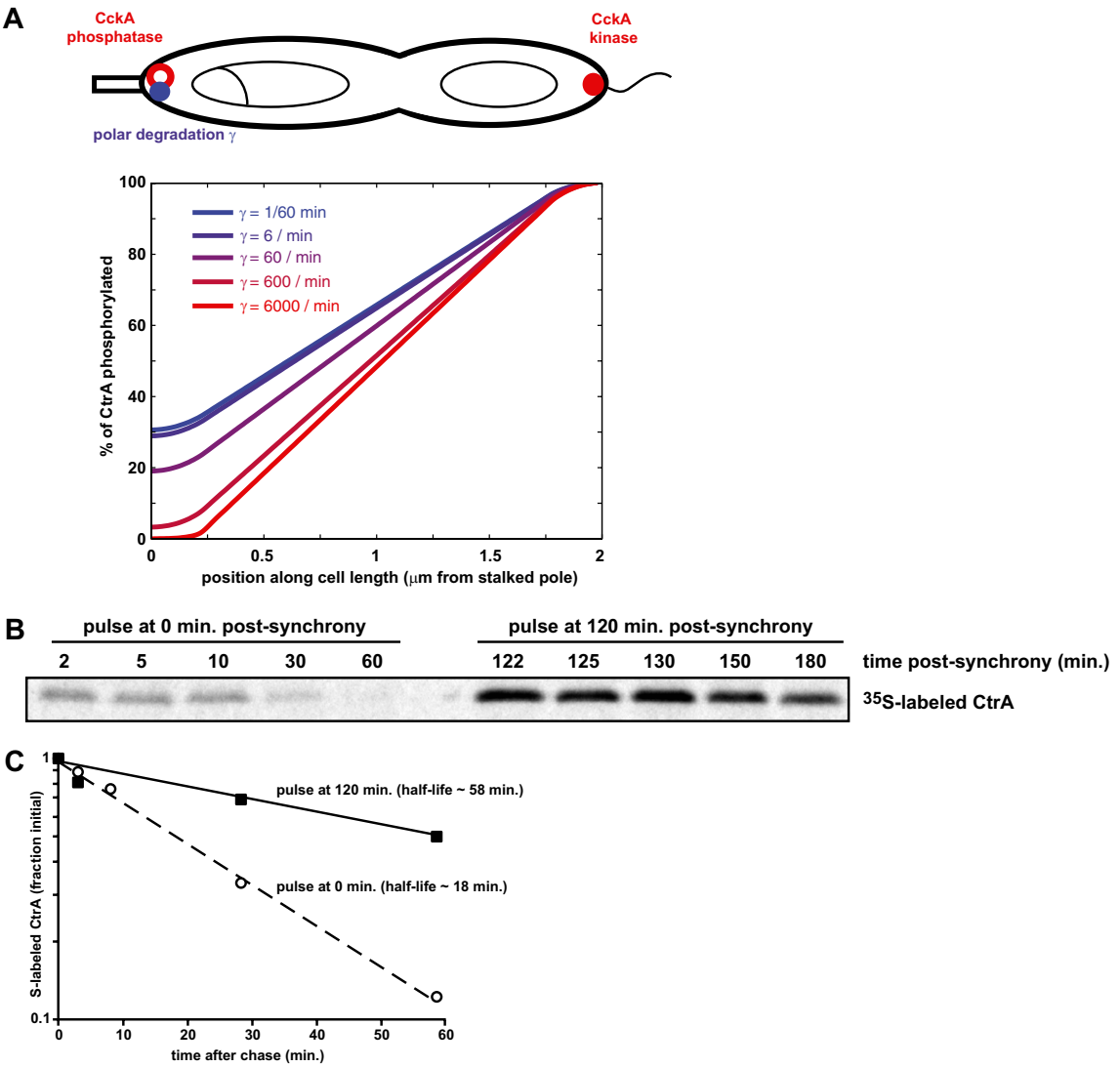

Fig. S7. CtrA proteolysis does not significantly contribute to the CtrA∼P gradient. (*A*) Mathematical modeling of the effects of CtrA proteolysis on the distributions of CtrA∼P using a 1D reaction–diffusion model; proteolysis (represented by the blue circle) is assumed to be concentrated at the stalked pole (details in *Materials and Methods*). For the experimentally measured CtrA half-life of 60 min (rate ≈0.0003/s), the spatial gradient generated by CckA-mediated phosphorylation with rate σ_k = 100/s and dephosphorylation with rate σ_p = 10/s is almost completely unaffected (purple curve). (*B*) Pulse-chase analysis of CtrA protein stability in synchronized cultures of wild-type CB15N. Swarmer cells were synchronized, released into fresh M2G, and CtrA stability measured either immediately or after 120 min. (*C*) Exponential fit to pulse-chase data from *A*. The half-lives of CtrA in cells pulsed immediately or 120 min after release into M2G were calculated to be 18 and 58 min, respectively.

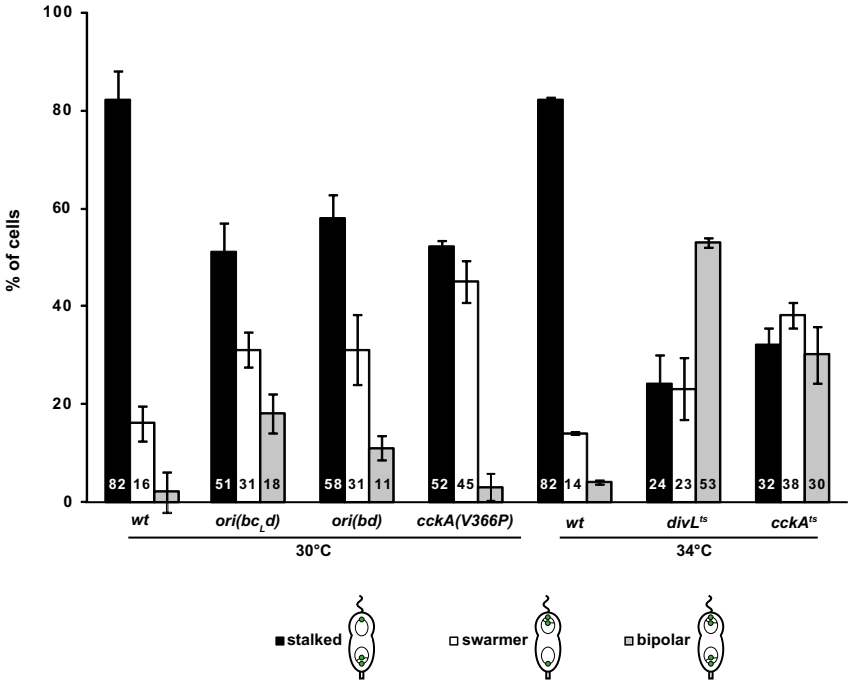

Fig. S8. Summary of spatial patterns of DNA replication. Quantification of DNA replication patterns in predivisional cells of the strains indicated. Error bars represent SDs for quantifications from three independent cultures, processed on 3 different days.

Table S1. Strains, plasmids, and primers

Organism or category	Name	Genotype, plasmid description, or primer sequence	Source
C. crescentus	CB15N	Synchronizable derivative of wild-type CB15	(1)
	GM3193	*ori*(bc_L*d*)	(2)
	GM3103	*ori(bd)*	(2)
	LS4259	pKR173 (pMR20:Pxyl-*YFP-ctrA*) ($gent^R$)	(3)
	MT16	*cc0006*::$(tetO)_n$ ($gent^R$) + *xylX*::*lacI-ECFP, tetR-EYFP* ($spec^R$) ($gent^R$, $spec^R$)	(4)
	PC4403	*divL346* (*divL*^{ts})	(5)
	ML1506	pJS14:Pxyl-ctrA ($chlor^R$)	(6)
	ML1681	*cckA-EGFP*::gent ($gent^R$)	(7)
	ML1753	*divL*^{ts}::chlor in MT16 ($chlor^R$, $spec^R$, $gent^R$)	This study
	ML1754	*cckA(V366P)* in MT16 ($spec^R$, $gent^R$)	This study
	ML1755	Δ*pleC*::tet in MT16 (tet^R,$spec^R$,$gent^R$)	This study
	ML1756	*divL-EGFP*::gent ($gent^R$)	This study
	ML1793	*ori*(bc_L*d*) + *cc0006*::$(tetO)_n$ ($gent^R$, kan^R) + *xylX*::*lacI-CFP, tetR-YFP* ($spec^R$) (kan^R, $gent^R$, $spec^R$)	This study
	ML1794	*ori(bd)* + *cc0006*::$(tetO)_n$ ($gent^R$, kan^R) + *xylX*::*lacI-CFP, tetR-YFP* ($spec^R$) (kan^R, $gent^R$, $spec^R$)	This study
	ML1795	*cckA*^{ts} in MT16 ($spec^R$, $gent^R$)	This study
	ML1798	*divL*^{ts}*::chlor* ($chlor^R$)	This study
	ML1876	*Pxyl-ftsZ* (kan^R) + *cc0006*::$(tetO)_n$ ($gent^R$) + *vanA*::*tetR-YFP* (kan^R, $gent^R$)	This study
E. coli	DH5a	General cloning strain	Invitrogen
	TOP10	Strain for constructing pENTR-TOPO clones	Invitrogen
General purpose vectors	pJS14	Derivative of pBBR1MCS, high-copy replicon ($chlor^R$)	Lab collection
	pJS71	Derivative of pBBR1MCS, high-copy replicon ($spec^R$)	Lab collection
	pML83	P_{xyl} oriented against P_{lac}, inserted into EcoRI site of pJS71 ($chlor^R$)	Lab collection
	pMR10	Broad host range, low copy vector (kan^R)	Lab collection
	pMR20	Broad host range, low copy vector (tet^R)	Lab collection
	pNPTS138	Integration vector (kan^R)	Lab collection
	pGFPC-4	Integration vector for c-terminal tagging of desired protein with EGFP ($gent^R$)	(8)
	pMCS-6	Integration vector ($chlor^R$)	(8)
Integration plasmids	pNPTS138:*cckA(V366P)*	For markerless allelic replacement of *cckA*	This study
	pNPTS138:*cc0006-tetO*	For integration of *tetO* cassette at *cc0006*, near the origin	This study
	pGFPC-4:*cckA-GFP*	For replacing *cckA* with *cckA-EGFP* on the chromosome	This study
	pGFPC-4:*divL-GFP*	For replacing *divL* with *divL-EGFP* on the chromosome	This study
	pMCS-6: *divL(A288V)*	For integration of *divL*^{ts} at the native locus	This study
Overexpression plasmids	pJS14:P_{xyl}-*ctrA*	High-copy plasmid, xylose-inducible expression of *ctrA* (pID42)	(6)
	pML83:P_{xyl}-*cckA(V366P)*	High-copy plasmid, xylose-inducible expression of *cckA(V366P)*	(7)
Primers	CckA_497_EcoRI_Fw	GAATTCtgcgggcggacggctgatga	This study
	CckA_1717_HindIII_Rev	AAGCTTtcgtcctcgacgaacaggat	This study
	CC0006_HindIII_fw	cagcagcagaagcttATGGCCCAGTTCCAGACCCT	This study
	M13R_EcoRI	cagcagcaggaattcCACAGGAAACAGCTATGA	This study
	divLfulllengthrev	cagcagcaggaattctcGAAGCCGAGTTCGGGCTGC	This study
	divLfwd1788	cagcagcagggtaccCGTGCTGGACATGGCCCA	This study

1. Evinger M, Agabian N (1977) Envelope-associated nucleoid from *Caulobacter crescentus* stalked and swarmer cells. *J Bacteriol* 132(1):294–301.
2. Bastedo DP, Marczynski GT (2009) CtrA response regulator binding to the *Caulobacter* chromosome replication origin is required during nutrient and antibiotic stress as well as during cell cycle progression. *Mol Microbiol* 72(1):139–154.
3. Iniesta AA, McGrath PT, Reisenauer A, McAdams HH, Shapiro L (2006) A phospho-signaling pathway controls the localization and activity of a protease complex critical for bacterial cell cycle progression. *Proc Natl Acad Sci U S A* 103:10935–10940.
4. Viollier PH, et al. (2004) Rapid and sequential movement of individual chromosomal loci to specific subcellular locations during bacterial DNA replication. *Proc Natl Acad Sci U S A* 101: 9257–9262.
5. Wu J, Ohta N, Zhao JL, Newton A (1999) A novel bacterial tyrosine kinase essential for cell division and differentiation. *Proc Natl Acad Sci U S A* 96:13068–13073.
6. Domian IJ, Quon KC, Shapiro L (1997) Cell type-specific phosphorylation and proteolysis of a transcriptional regulator controls the G1-to-S transition in a bacterial cell cycle. *Cell* 90: 415–424.
7. Chen YE, Tsokos CG, Biondi EG, Perchuk BS, Laub MT (2009) Dynamics of two phosphorelays controlling cell cycle progression in. *Caulobacter crescentus. J Bacteriol* 191:7417–7429.
8. Thanbichler M, Iniesta AA, Shapiro L (2007) A comprehensive set of plasmids for vanillate- and xylose-inducible gene expression in *Caulobacter crescentus*. *Nucleic Acids Res*, 10.1093/nar/gkm818.